Cite this article
Gradišar Centa U, Sterniša M, Višić B *et al.* (2021)
Novel nanostructured and antimicrobial PVDF-HFP/PVP/MoO_3 composite.
Surface Innovations **9(5)**: 256–266,
https://doi.org/10.1680/jsuin.20.00073

Invited Feature Article
Paper 2000073
Received 01/10/2020; Accepted 08/12/2020
Published online 15/12/2020

Keywords: anti-bacterial/nanocomposites/surface characterisation

Surface Innovations

ice Publishing

Novel nanostructured and antimicrobial PVDF-HFP/PVP/MoO_3 composite

Urška Gradišar Centa MSc
PhD student, Condensed Matter Physics Department, Jožef Stefan Institute, Ljubljana, Slovenia (Orcid:0000-0001-5206-141X) (corresponding author: urska.gradisar@ijs.si)

Meta Sterniša PhD
Teaching Assistant and Researcher, Department of Food Science and Technology, Biotechnical Faculty, University of Ljubljana, Ljubljana, Slovenia (Orcid:0000-0002-2414-3618)

Bojana Višić PhD
Assistant Research Professor, Solid State Physics Department, Institute of Physics Belgrade, Belgrade, Serbia; Center for Solid State Physics and New Materials, Jožef Stefan Institute, Ljubljana, Slovenia (Orcid:0000-0002-2065-0727)

Žiga Federl BSc
Student, Faculty of Mathematics and Physics, University of Ljubljana, Ljubljana, Slovenia

Sonja Smole Možina PhD
Professor, Department of Food Science and Technology, Biotechnical Faculty, University of Ljubljana, Ljubljana, Slovenia (Orcid:0000-0001-7949-8128)

Maja Remškar PhD
Professor, Condensed Matter Physics Department, Jožef Stefan Institute, Ljubljana, Slovenia (Orcid:0000-0002-8919-1768)

Contact surfaces represent a liability for the transmission of microbial contamination, leading to high consumption of detergents and biocides for their care and further increasing the already problematic antimicrobial resistance of microorganisms. This issue could be addressed by the use of antimicrobial nanocomposite coatings. In this research, a polymer nanocomposite of inert poly(vinylidene fluoride-*co*-hexafluoropropylene) (PVDF-HFP) and water-soluble polyvinylpyrrolidone (PVP) polymers with molybdenum trioxide (MoO_3) nanowires (NWs) was designed and characterised for to its surface properties and antimicrobial potential. The nanocomposite has an inhomogeneous structure with a positively charged and hydrophilic surface. The nanofiller reduces the surface roughness, changes the zeta potential from negative to positive, increases the wetting angle and thermal stability of the blend and maintains the polar β-phase in PVDF-HFP. The high specific surface area of the NWs leads to rapid release into water and causes pH decrease, followed by hydrolysis of PVP polymer and formation of carboxyl acid and ammonium salt. The antimicrobial activity of the nanocomposite inactivates both bacteria and fungi, indicating that the novel nanocomposite is a stable nanostructured coating unfavourable for microorganism colonisation. The antimicrobial activity of this nanocomposite is activated by water, which makes it an intriguing candidate for antimicrobial coating of contact surfaces.

Notation

A	surface area of the foils
C	average number of cells counted
D	dilution factor
E	electric field
E^*	elastic modulus
N	number of viable cells per square centimetre of the tested foil
R_a	average surface roughness of the foils
$\tan \delta$	loss tangent
T_s	sample temperature
V	volume of the solution used to wash the foils
v	measured electrophoretic velocity
ε	electrical permittivity of the electrolytic solution
η	viscosity
ζ	zeta potential

1. Introduction

Contact surfaces pose a risk for the transmission of microbial contamination. Moisture from the air and organic molecules created by frequent contact with hands provides the right environment for microorganisms to colonise, grow and form a biofilm. In order to survive, microorganisms form biofilms that protect them from the negative effects of the environment, including biocides.[1] Antimicrobial coatings are a promising approach to preventing the adhesion and growth of microorganisms on different surfaces in hospitals and other public spaces (e.g. door handles, passenger hand straps on buses, buttons in elevators, handrails of shopping carts, tables in dining rooms and work surfaces in kitchens).[2] Therefore, the development of new surface treatments has become a topic of great interest, and more attention is being paid to the development of antimicrobial coatings.

Various synthetic approaches based on the immobilisation of microbes or the release of antimicrobial substances, such as metal derivatives and nanomaterials, polyammonium salts, natural antimicrobials and antibiotics, have been used in antimicrobial coatings.[3–7] However, the increasing problem of growing microbial resistance to antimicrobial agents has led to the search for new ones with a non-specific mechanism of action that can be achieved by using different metals. Silver (Ag), zinc (Zn) and titanium (Ti) and their oxides have been extensively studied for such purposes. When inorganic nanoparticles are incorporated into polymer nanocomposites, their physico-chemical properties

differ from those of the individual components and lead to the development of novel multifunctional materials with a variety of applications, including the possibility of use as an antimicrobial coating. For example, polymer/nanosilver composite multilayer coatings have shown controlled release of biocidal silver ions and relatively good biocompatibility and environmental safety.[8] Biocompatible poly(*N*-isopropylacrylamide) coatings with incorporated zinc oxide (ZnO) nanoparticles were reported as an alternative to nanosilver. These showed a bactericidal behaviour towards *Escherichia coli* at a low zinc oxide concentration (approximately 0.74 μg/cm^2).[9] Nanotitania/polyurethane composite coatings also showed antibacterial activity against *E. coli*, as 99% of the bacteria were inactivated in less than 1 h under solar irradiation.[10] Unfortunately, silver and zinc oxide nanoparticles are toxic to human cells,[11] while ultraviolet (UV) light is needed to activate the antimicrobial properties of titanium dioxide (TiO_2).[10]

Various molybdenum (Mo) oxides have already been proposed as an alternative to these inorganic particles for use in public and healthcare environments because of their low cytotoxicity, biocompatibility and good antimicrobial activity.[12] A good antimicrobial potential of molybdenum oxides has also been shown in other studies.[13–17] The antimicrobial activity has been attributed to an acidic surface reaction in the presence of water that produces molybdic acid, which dissociates into hydronium (H_3O^+) and molybdate (MoO_4^{2-}) ions.[14] Moreover, antimicrobial activity has been shown to be dependent on the energy gap of molybdenum trioxide (MoO_3) nanorods[15] and on a specific molybdenum trioxide crystallographic phase.[12] A further comparison of commercial and synthesised forms showed the better activity of the synthesised orthorhombic structure.[12]

In addition to the antimicrobial potential of the nanofiller used for the antimicrobial composite, the properties of novel nanocomposite coating must also meet other requirements. The embedded nanomaterials (or the ions dissolved from them) need to come into physical contact with the bacteria to affect them, and part of the host material must be chemically inert to form the coating matrix. Therefore, a mixture of a water-soluble polymer containing water-soluble nanomaterials and water-insoluble polymers as the coating matrix would be a preferred design.

Within the scope of this research, a polymer nanocomposite was designed from a mixture of poly(vinylidene fluoride-*co*-hexafluoropropylene) (PVDF-HFP) and water-soluble polyvinylpyrrolidone (PVP) polymers with the addition of molybdenum trioxide nanowires (NWs). PVDF-HFP was chosen as the chemically inert part of the nanocomposite, characterised by low crystallinity (approximately 50%), low-temperature glass transition (−35°C) and high thermal stability (up to 143°C).[18–21] PVP is a biocompatible and water-soluble polymer with low chemical toxicity, high water solubility and the ability to act as a dispersant.[22] This particular combination of polymers has been reported as a possible novel high-temperature proton-exchange membrane[23] and for applications in wound healing.[24] Modified PVDF-HFP membranes with grafting of *N*-vinyl-2-pyrrolidone and iodine (I) immobilisation[22] and quaternised pyridinium groups[25] have been shown to have good antimicrobial activity.

The nanocomposite was prepared in the form of a thin, self-standing foil as a model of a contact coating. The surface morphology on the nanoscale, the structural properties and the wetting angle, as well as the optical vibration and dynamic mechanical properties, were evaluated, and the antimicrobial activity of this nanocomposite against bacteria and fungi was determined.

2. Experimental section

2.1 Nanomaterial used and preparation of the nanocomposite

Molybdenum trioxide NWs with a diameter of 100–150 nm and a length of up to 3 μm have a high degree of porosity and a specific surface area of 12 m^2/g. They are synthesised by oxidation of $Mo_6S_2I_8$ NWs (Nanotul Ltd, Slovenia) at 285°C for 24 h.[26] Molybdenum trioxide NWs grow in an orthorhombic crystal structure (JCPDS 76-1003). The solubility of molybdenum trioxide is 2.03 ± 0.09 mg/ml in pure water. The authors showed that 6 h exposure of HaCaT cells to molybdenum trioxide at a concentration of 1 mg/ml had no effect on the survival of these cells – that is, no cytotoxic effect was observed.[27]

For the preparation of the nanocomposite, PVDF-HFP, from Sigma-Aldrich, USA, and PVP K30, from Sigma-Aldrich, USA, were dissolved separately in dimethylformamide (DMF), from Carlo Erba Reagents, Italy, and mixed using a magnetic stirrer for 2 h at 400 revolutions per min (rpm) at 80°C. In the next step, the molybdenum trioxide NWs were added to PVP and the dispersion was mixed for 2 h. Finally, PVP with molybdenum trioxide was mixed with the dissolved PVDF-HFP for another 2 h. The same mass ratio of 69:23:8 (PVDF-HFP:PVP:molybdenum trioxide) was used to prepare all foils. They were prepared by casting of the nanocomposite solution onto a Teflon plate and drying for 2 h at 80°C. For comparison, a PVDF-HFP/PVP polymer blend without molybdenum trioxide was prepared by mixing (2 h) separately dissolved polymers in DMF and then cast and dried under the same conditions as the PVDF-HFP/PVP/molybdenum trioxide nanocomposite.

2.2 Physico-chemical characterisation

The morphology of the nanocomposite films was investigated with a Supra 36 VP field-emission scanning electron microscope (SEM), from Carl Zeiss, Germany. The samples were placed on adhesive carbon (C) tape and sputtered with a 10 nm gold (Au) layer, with the aim of increasing the conductivity of the electrons during the investigation. The Raman spectra and the topography of the nanocomposites were recorded with an alpha300 confocal Raman microscope from WITec, Germany, using green laser (532.3 nm) and equipped with an atomic force microscope (AFM). The power of the laser beam measured on the sample was 0.3 mW.

The concentration of molybdenum trioxide dissolved from the nanocomposite foils was determined by UV–Vis spectroscopy using a PerkinElmer Lambda 950 spectrometer (USA) and a quartz cuvette. The nanocomposite foil with a mass concentration of 5 mg/ml was added to water in a glass beaker at room temperature (RT) while mixed with a magnetic stirrer at 300 rpm for 6 h. For the calibration curve, the absorbance amplitude of the peak at 210 nm in several molybdenum trioxide–water solutions with known concentrations was used. The surface zeta potential was measured with an Anton Paar SurPass electrokinetic analyser (Austria) with an adjustable gap cell and sample dimensions of 20 × 10 mm. The time for four measuring cycles was 5 min. The electrolyte used was a 0.001 M potassium chloride (KCl) solution in ultrapure water. The zeta potential was automatically calculated from the electrophoretic mobility, based on the Smoluchowski equation, $v = (\varepsilon E/\eta)\xi$, where v is the measured electrophoretic velocity, η is the viscosity, ε is the electrical permittivity of the electrolytic solution and E is the electric field.[28]

The wetting angle of the coatings for distilled water was measured at three points of each sample with an optical tensiometer Attension Theta Lite TL100 (Sweden) and the sessile drop method. All measurements were performed at RT, and the results are presented as the mean value with the associated standard deviation. The dynamic contact angle (CA) of water on the polymer blend and nanocomposite foil was determined according to the Wilhelmy plate method[29] with a Krüss K100 processor tensiometer (Krüss, Germany). The surface tension of demineralised water was obtained from the Krüss LabDesk database (72.8 mN/m).[30] A new sample and fresh water were used for each test cycle. The sample was first immersed in the liquid with the film normal perpendicular to the direction of immersion and then pulled out in reverse. The measurement began when the liquid buoyancy force acting on the sample was first detected and the sample reached an immersion depth of 2 mm. The immersion speed and pull-out speed were 6 mm/min. The sensitivity of force detection was set to 0.001 N. The maximum immersion depth was 7 mm. The advancing and receding CAs were determined with the Krüss LabDesk software.

The pH values were measured with a SevenExcellence multiparameter meter, from Mettler Toledo, Switzerland, with an InLab Expert Pro-ISM probe. The polymer blend and the nanocomposite foil with a mass concentration of 5 mg/ml were added to water in a glass beaker at RT. The samples were mixed with a magnetic stirrer at 300 rpm, and the pH was measured at 1 min intervals. While dissolving, they were submerged under the water surface.

The dynamic mechanical properties of the coatings were investigated with a DMA/SDTA861 dynamic mechanical analyser, from Mettler Toledo, Switzerland, in tension mode. The validity of Hooke's law – that is, the range in which the material behaves elastically – was measured with a displacement between 1 and 20 µm.

2.3 Antimicrobial test

The antimicrobial activity against Gram-positive bacteria (*Staphylococcus aureus* ŽMJ72 and *Listeria monocytogenes* ŽM58), Gram-negative bacteria (*E. coli* ŽM370 and *Pseudomonas aeruginosa* ŽM519), yeasts (*Candida albicans* ŽMJ32 and *Pichia anomala* ŽMJ6) and moulds (*Penicillium verrucosum* ŽM23 and *Aspergillus flavus* ŽM25) was evaluated. All microorganisms were from the culture collection of the Laboratory for Food Microbiology at the Department of Food Science, Biotechnical Faculty (designations ŽM and ŽMJ). The bacteria were stored in tryptic soy broth (Biolife, Italy) and the fungi in malt extract broth (Biolife, Italy) with 15% glycerol (Kemika, Croatia) at −80°C, revitalised on tryptic soy agar (TSA; Biolife, Italy) or malt extract agar (MEA; Biolife, Italy) and incubated at 37°C for 24 h for the bacteria or at 30°C for the yeasts and at 25°C for 5–7 days for the moulds (I-105 CK incubator, Kambič, Slovenia). Standardised inocula with a cell concentration of 5 log colony-forming units (CFU)/ml were prepared.

The antimicrobial potential of the material was evaluated using a modified ISO 22196 method.[31] An inert foil (polyethylene (PE)) was used as negative control, while the PVDF-HFP/PVP polymer blend was used for comparison with the PVDF-HFP/PVP/molybdenum trioxide nanocomposite. The inoculum of individual bacteria, yeast or mould was applied to PE, the PVDF-HFP/PVP polymer blend and the PVDF-HFP/PVP/molybdenum trioxide nanocomposite foils and covered with a PE foil to keep them humid. All three foil types were tested in three parallel experiments. After the test periods (0, 3 and 6 h for all test microorganisms and an additional 24 h for the fungi), the microorganisms were washed from the coatings with a neutraliser (soybean casein digest broth with lecithin and polyoxyethylene sorbitan monooleate), mixed on an orbital shaker for 10 min, diluted in saline solution and plated using the pour plate method with TSA for the bacteria and MEA for the fungi. The number of viable cells was calculated as $N = (100 \times C \times D \times V)/A$, where N is the number of viable cells per square centimetre of the tested foil, C is the average number of cells counted, D is the dilution factor, V is the volume of the solution used to wash the foils (10 ml) and A is the surface area of the foils (400 mm^2). The results for each microorganism at each time point were compared with analysis of variance and post hoc Tukey test in the SPSS software program.

3. Results

3.1 Surface topography of the PVDF-HFP/PVP blend and PVDF-HFP/PVP/molybdenum trioxide nanocomposite

The surface topography of the investigated materials is shown in Figure 1. The molybdenum trioxide NWs have relatively homogeneous sizes, with a length of up to a few micrometres and a diameter of 100–150 nm (Figure 1(a)). The surface of the PVDF-HFP/PVP blend (Figure 1(b)) is nanostructured with rounded PVP islands with diameters of 200–500 nm. The PVDF-HFP/PVP/molybdenum trioxide nanocomposite (Figure 1(c)) has

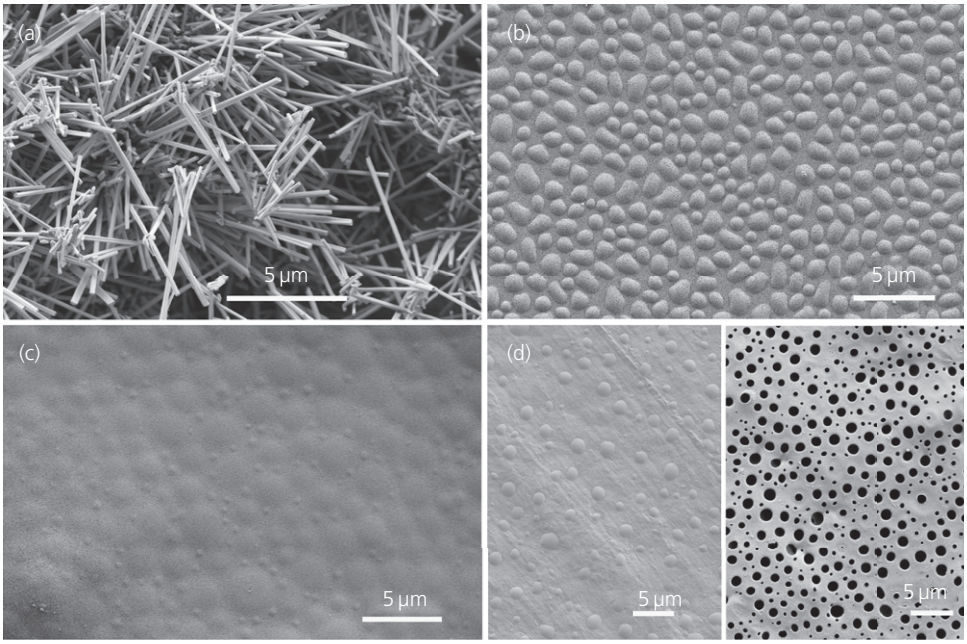

Figure 1. SEM images of (a) molybdenum trioxide NWs, (b) PVDF-HFP/PVP polymer blend, (c) PVDF-HFP/PVP/molybdenum trioxide nanocomposite and (d) PVDF-HFP/PVP polymer blend after 6 h in water and (e) PVDF-HFP/PVP/molybdenum trioxide nanocomposite after 6 h in water

a domain surface structure with a diameter of a few micrometres and PVP islands in the submicrometre range. After 6 h exposure of the polymer blend and the nanocomposite foils to water, partial removal of the PVP islands from the surface of the polymer blend was observed (Figure 1(d)), but they were completely removed from the surface of the molybdenum trioxide nanocomposite, leaving a porous surface (Figure 1(e)).

The surface topography of the polymer matrix (Figure 2(a)) and the polymer nanocomposite (Figure 2(b)) on the nanometre scale was revealed using an environmental AFM. The bright PVP islands in the matrix are about 200 nm high, whereas in the nanocomposite, the height was twice reduced and smaller islands are visible. The addition of molybdenum trioxide NWs reduced the surface roughness of the polymer nanocomposite with respect to that of the polymer matrix.

3.2 Vibration analysis of the PVDF-HFP/PVP blend and PVDF-HFP/PVP/molybdenum trioxide nanocomposite

Raman spectroscopy was used to study the polymer blend (Figure 3(a)) and the effect of molybdenum trioxide NWs (Figure 3(b)) on their vibration states. The positions of the Raman peaks are listed in Tables 1 and 2 and attributed to specific components. It is important to note that the Raman peak at 839 cm^{-1} indicates the presence of the polar β-phase of PVDF-HFP,[34] which increased strongly in the polymer blend (Figure 3(a), spectrum C). In the spectrum recorded between the PVP islands (Figure 3(b),

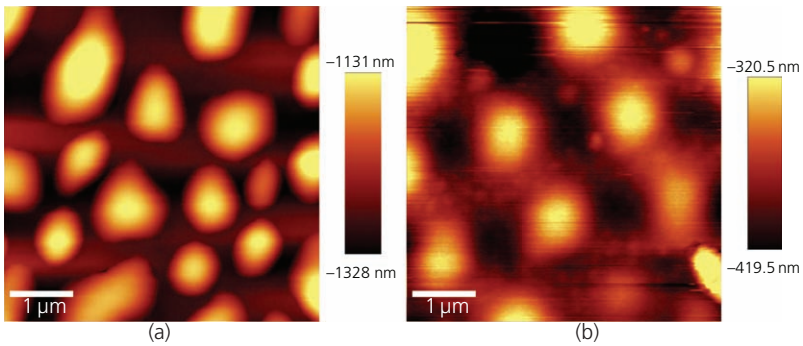

Figure 2. AFM images: (a) PVDF-HFP/PVP polymer blend; (b) PVDF-HFP/PVP/molybdenum trioxide nanocomposite

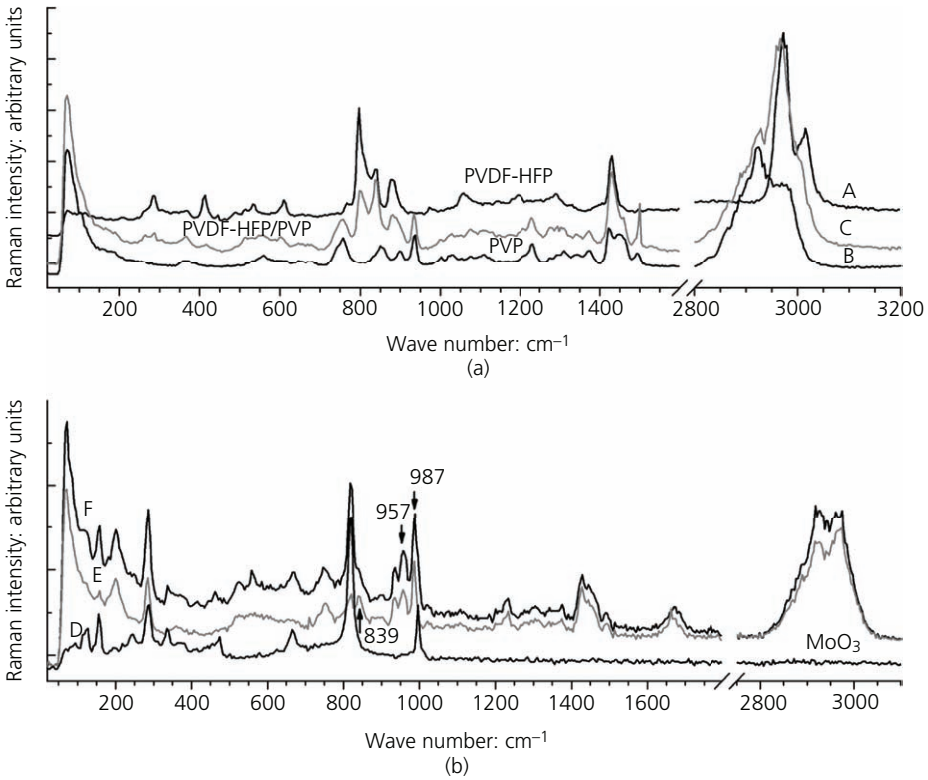

Figure 3. Raman spectra: (a) polymers (A, PVDF-HFP; B, PVP) and polymer blend (C, PVDF-HFP/PVP); (b) molybdenum trioxide (D) and PVDF-HFP/PVP/molybdenum trioxide nanocomposite (E, between islands; F, island)

Table 1. Positions of Raman peaks in the spectra of the PVDF-HFP/PVP blend, pure PVP and pure PVDF-HFP

PVDF-HFP/PVP blend		PVP		PVDF-HFP	
Position: cm^{-1}	Relative intensity: %	Position: cm^{-1}	Literature[32,33]	Position: cm^{-1}	Literature[28]
71	100	70	72	—	—
285	78	—	—	283	284
558	63	560	556	413	—
747	64	—	746	610	—
757	53	758	758	797	—
839	63	850	—	839	839 β-phase
—	—	898	—	—	—
—	—	—	—	876	—
934	53	937	934		—
—	—	—	—	1058	—
—	—	—	—	1194	
1233	50	1232	1233, 1228	—	—
—	—	—	—	1290	—
1429	62	1422	1421	—	1430
1445	59	1447	—	—	1445
1490	53	1492	1494	—	—
1668	54	1660	1665, 1663	—	—
2924	78	2922	2928	—	—
2974	78	2969	—	2972	2971
—	—	—	—	3015	—

spectrum E), the presence of the molybdenum trioxide peaks is less expressed than in the spectrum recorded on the PVP islands (Figure 3(b), spectrum F), where the molybdenum trioxide peaks dominate. This indicates that most of the molybdenum trioxide is located on the PVP islands. The polar β-phase in PVDF-HFP is distinctive in spectrum E (between the islands), while in spectrum F (on the islands), it appears as a weak shoulder on the strong molybdenum trioxide peak centred at 819 cm^{-1}. However, in both

Table 2. Position of Raman peaks in the spectra of the PVDF-HFP/PVP/molybdenum trioxide nanocomposite taken on the PVP islands, on the area between the PVP islands and on pristine molybdenum trioxide NWs, with peaks assigned

Islands		Between islands		Molybdenum trioxide			Assignment
				This study		Literature[34–36]	
Position: cm^{-1}	Relative intensity: %	Position: cm^{-1}	Relative intensity: %	Position: cm^{-1}	Relative intensity: %	Position: cm^{-1}	
72	100	72	100				PVP
124	60	124	72	127	64	130	Molybdenum trioxide
158	74	158	70	156	69	159–161	Molybdenum trioxide
201	73	200	73	197	58	199	Molybdenum trioxide
217	sh	217	sh	218	59	219	Molybdenum trioxide
248	sh	249	sh	246	62	249	Molybdenum trioxide
286	78	285	73	289	71	295	PVDF-HFP, molybdenum trioxide
337	59	—	—	335	64	339–340	Molybdenum trioxide
474	56	—	—	474	61	470–482	Molybdenum trioxide
668	62	—	—	665	63	666–667	Molybdenum trioxide
817	85	821	69	821	100	820–823	Molybdenum trioxide
839	63	839	68	—	—	—	PVDF-HFP β-phase
935	64	935	68	—	—	—	PVP
957	68	957	70	—	—	—	New peak
987	77	987	78	—	—	—	New peak

sh, peak shoulder

nanocomposite spectra (E and F), two new peaks are observed at 957 and 987 cm^{-1}. The peak at 957 cm^{-1} is assigned to O=Mo=O symmetric polarised stretching modes,[32] while the narrow intense peak at 987 cm^{-1} is generally assigned to the terminal oxygen (Mo^{6+}=O) stretching mode.[33,35,36]

3.3 Mechanical properties of the PVDF-HFP/PVP blend and PVDF-HFP/PVP/molybdenum trioxide nanocomposite

The curves of the elastic modulus (E^*) and the loss tangent (tan δ) of the polymer blend (a, b) and the polymer nanocomposite (c, d) are shown in Figure 4. The spectra are rather featureless, with broad glass-transition peaks at −55 ± 3°C (full width at half maximum

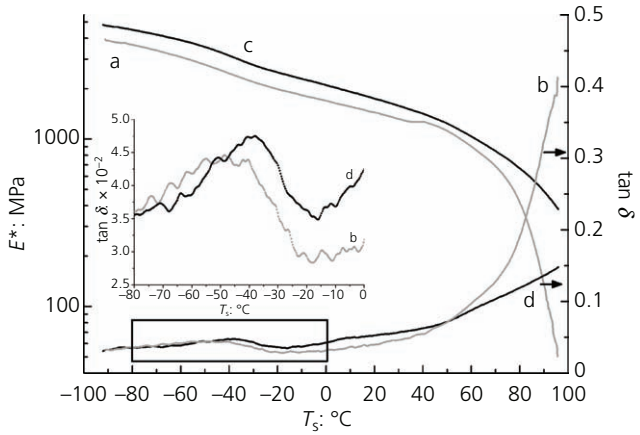

Figure 4. Elastic modulus E^* and tan δ: a, b, PVDF-HFP/PVP blend; c, d, PVDF-HFP/PVP/molybdenum trioxide nanocomposite

(FWHM): 37 ± 1°C) (blend) and at −38 ± 3°C (FWHM: 26 ± 1°C) (nanocomposite). The broadness of the peaks indicates the inhomogeneity of the polymer blend. The smaller FWHM of the convolution peak of the nanocomposite indicates that the molybdenum trioxide filler reduces the degree of inhomogeneity, corresponding to the smoother surface of the nanocomposite in relation to that of the pure polymer blend revealed by the AFM (Figure 2). The related glass-transition temperatures of the constituent polymers are −35°C (PVDF-HFP[19]) and 170°C (PVP[37]). For PVDF-HFP, a transition temperature of 50°C was also observed.[19] Above this temperature (50°C), where the tan δ curves in Figure 4 intersect, the pure polymer blend entered the elastic flow region, while the nanocomposite shows higher thermal stability with a rubber-like plateau extending to the final temperature (95°C) of the measurement. This thermal stabilisation of the PVDF-HFP part of the blend by the molybdenum trioxide nanofiller is evidence of the interaction between the molybdenum trioxide NWs and the PVDF-HFP chains during crystallisation of the polymer blend.[38] The addition of molybdenum trioxide to the polymer blend increased the complex elastic modulus E^* of the polymer nanocomposite over the entire temperature range.

3.4 Wetting angle and surface charge of the PVDF-HFP/PVP blend and PVDF-HFP/PVP/molybdenum trioxide nanocomposite

The degree of the surface hydrophilicity of the PVDF-HFP/PVP blend and the PVDF-HFP/PVP/molybdenum trioxide nanocomposite foils was investigated by static and dynamic CA measurements. Figure 5 shows the water CAs of the polymer blend (Figure 5(a)) and the polymer nanocomposite (Figure 5(b)). The molybdenum trioxide NWs increased the CA of the nanocomposite (87.1 ± 0.1°) compared with that of the polymer blend (83.5 ± 0.1°). The surfaces

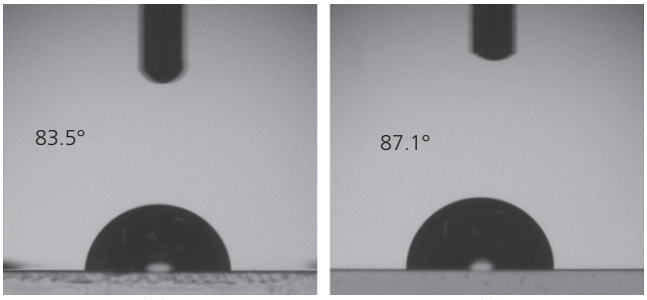

Figure 5. CA test: (a) PVDF-HFP/PVP polymer blend; (b) PVDF-HFP/PVP/molybdenum trioxide nanocomposite

of the samples are chemically heterogeneous and have nanostructures at the atomic scale. For this reason, the dynamic CA was also measured using the Wilhelmy plate method.[39] The advancing CA was 87.5 ± 0.2° for the nanocomposite and 83.8 ± 0.2° for polymer blend. In both cases, the receding CA was 0°. The addition of nanoparticles can modify the wettability of polymer surfaces, as they can alter the chemical composition of the surface or the surface morphology – for example, surface roughness.[40] The surface roughness of the nanocomposite was twice smaller than that of the polymer blend, and therefore, the authors observed a slightly larger value of the CA. Increasing the surface roughness decreases the CA.[41] The values of the advancing angles indicate that the nanocomposite is slightly less hydrophilic than the pure polymer blend, although it can still be considered hydrophilic (CA < 90°).

Table 3. Results and parameters of the zeta-potential measurements

	pH	Zeta potential: mV	Gap height: µm
PVDF-HFP/PVP polymer blend	6.57 ± 0.02	–26.3 ± 0.6	98.04
PVDF-HFP/PVP/molybdenum trioxide nanocomposite	5.62 ± 0.01	+ 10 ± 3	100.57

Since the electric charge of a material surface is considered one of the most important physical factors influencing biological interactions,[42] the surface charges of the PVDF-HFP/PVP blend and the PVDF-HFP/PVP/molybdenum trioxide nanocomposite were determined (Table 3). It was found that the polymer blend without molybdenum trioxide is negatively charged, while the addition of molybdenum trioxide NWs causes a change in the surface zeta potential to a positive value.

3.5 Solubility kinetics of the PVDF-HFP/PVP blend and PVDF-HFP/PVP/molybdenum trioxide nanocomposite in water

The polymer blend of water-soluble PVP and water-insoluble PVDF-HFP and the polymer nanocomposite PVDF-HFP/PVP with added water-soluble molybdenum trioxide at a concentration of 5 mg/ml were added to distilled water at RT, and the pH of the solutions was measured every minute for 340 min. The pH values of the solutions are shown in Figure 6(a). In the case of the polymer blend without molybdenum trioxide (curve A), the pH value reached a saturation value of 5.3 in 90 min. In the case of the molybdenum trioxide nanocomposite (curve B), the pH value dropped to 4.6 in the first 5 min and approached 3.8 after 6 h. The temporal development of the concentration of dissolved molybdenum trioxide NWs is presented in Figure 6(b). After a relatively short time, about 90 min, the concentration of molybdenum trioxide dissolved from the nanocomposite reached a saturation value of 0.09 mg/ml.

3.6 Antimicrobial activity

The antimicrobial properties of the PVDF-HFP/PVP/molybdenum trioxide nanocomposite were tested against Gram-positive bacteria *S. aureus* and *L. monocytogenes* (Figure 7(a)), Gram-negative

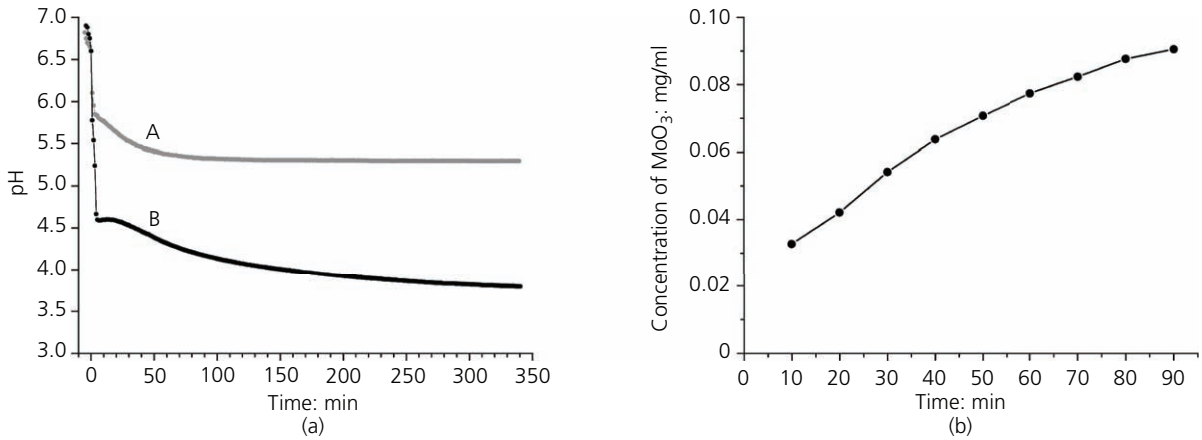

Figure 6. (a) Time evolution of pH values during dissolution in water of the PVDF-HFP/PVP blend (curve A) and PVDF-HFP/PVP/molybdenum trioxide nanocomposite (curve B); (b) concentration of dissolved molybdenum trioxide from the nanocomposite

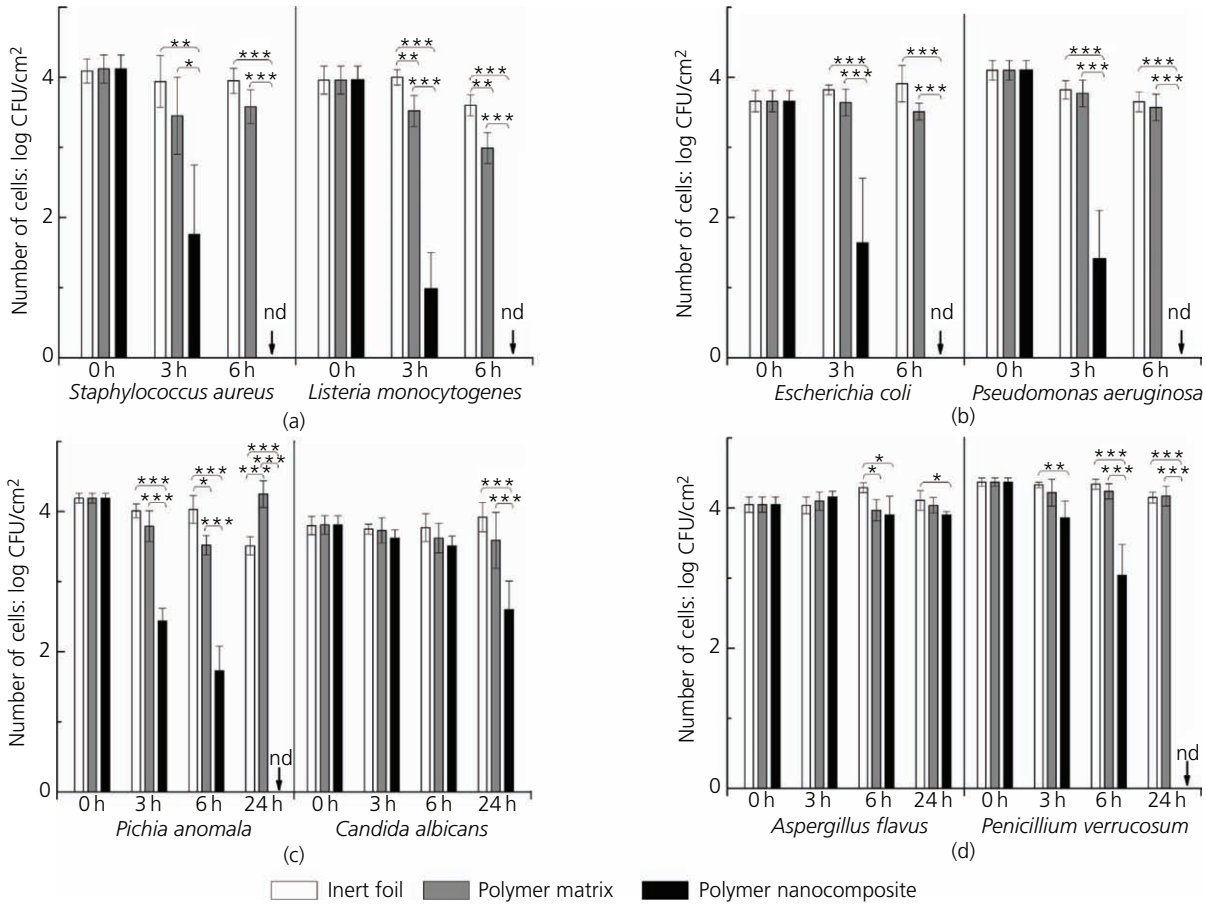

Figure 7. Kinetics of the antimicrobial activity of inert PE foil (empty columns), PVDF-HFP/PVP blend (grey columns) and PVDF-HFP/PVP/molybdenum trioxide nanocomposite (black columns) against (a) Gram-positive bacteria (*S. aureus* and *L. monocytogenes*), (b) Gram-negative bacteria (*E. coli* and *P. aeruginosa*), (c) yeasts (*C. albicans* and *P. anomala*) and (d) moulds (*P. verrucosum* and *A. flavus*). The abbreviation 'nd' means that the presence of microorganism was not detected. Asterisks indicate statistically significant difference (*$p < 0.05$; **$p < 0.01$; ***$p < 0.001$) between the compared parameters for each microorganism at a given time

bacteria *E. coli* and *P. aeruginosa* (Figure 7(b)), yeasts *C. albicans* and *P. anomala* (Figure 7(c)) and moulds *P. verrucosum* and *A. flavus* (Figure 7(d)). An inert PE foil was used as the negative control. A pure PVDF-HFP/PVP polymer blend was also tested and showed a statistically significant reduction in *L. monocytogenes* after 3 and 6 h. A reduction was also observed in *P. anomala* and *A. flavus* after 6 h, but these differences were no longer present after 24 h.

The antimicrobial activity of the PVDF-HFP/PVP/molybdenum trioxide nanocomposite was more pronounced against bacteria compared with that against fungi. The reduction trend in the number of colonies is evident for all four tested bacteria with a statistically significant reduction of 2–3 log after 3 h of incubation and with a complete bactericidal effect in 6 h (Figures 7(a) and 7(b)). For the yeasts, the antimicrobial effect was stronger against *P. anomala*, with statistically significant reductions of 1.7 log and 2.5 log in 3 and 6 h of incubation, respectively, and a fungicidal effect in 24 h (Figure 7(c)). The number of colonies of *C. albicans* was reduced less, but a statistically significant reduction of 1.2 log in 24 h was achieved (Figure 7(c)). Species-specific differences in antimicrobial activity were also observed in the moulds, where the nanocomposite reduced the number of *P. verrucosum* already after 3 h with a reduction of 0.5 log in 3 h and by 1.3 log in 6 h in a statistically significant way and showed a fungicidal effect in 24 h. In the case of *A. flavus*, however, this difference was observed after 6 and 24 h (Figure 7(d)).

4. Discussion

The growth of microbes on different surfaces depends on several physical and chemical conditions. The most important physical conditions are the appropriate temperature, pH value, surface topography and the presence of water, while the most important chemical condition is the availability of nutrients. The physical properties of the surface, such as topography, wetting angle and surface zeta potential, influence the adhesion of microbes and their interaction with the surface. The surface roughness (R_a) of the investigated foils determined with AFM was 420 nm for the PVDF-HFP/PVP blend and half (210 nm) for the PVDF-HFP/

PVP/molybdenum trioxide nanocomposite. It is already known that a small increase in the average surface roughness (R_a) value reduces bacterial adhesion.[43] The addition of molybdenum trioxide NWs to the PVDF-HFP/PVP blend causes a slightly higher CA of the PVDF-HFP/PVP/molybdenum trioxide nanocomposite. Nevertheless, both foils retain their hydrophilic character, which is unfavourable for the attachment of microorganisms.[44] The existence of the β-phase of PVDF-HFP both in the pure polymer blend and in the nanocomposite is explained by an interaction between the $>CF_2$ group of PVDF and the carbonyl groups of PVP, as reported for the case of esters.[45]

Both PVP and molybdenum trioxide are water soluble and lower the pH value of the solutions towards the acidic region. The slightly acidic solution of PVP is explained by the carboxyl groups that are located at the beginning of each PVP chain.[46] The high specific surface area of molybdenum trioxide NWs leads to a very rapid dissolution in water. In the first step, molybdic acid is formed, which then dissociates further to form molybdate and hydroxonium ions.[13] The acidic environment of the dissolving molybdenum trioxide NWs intensifies the hydrolysis reaction of the PVP polymer. It has been reported that the rate constant of the hydrolysis/hydration reaction of PVP in water increases with acidity.[46] The dependence of the co-operative solubility is evident from the time dependence of the pH value, which in the case of a polymer blend solution reached the final pH value (5.3) in 1.5 h, while it decreased steadily to 3.8 in 6 h due to the dissolution of the nanocomposite. The solubility also influences the distribution of the surface charge. The zeta potential of the polymer blend is −26.3 mV, indicating the presence of negatively charged ions during the dissolution of PVP. The addition of molybdenum trioxide NWs to the polymer blend causes a change in the zeta potential from negative to positive, probably due to the protonation of the carboxylate anions. The interaction between the molybdenum trioxide NWs and the PVP polymer is also evident in the emergence of two new Raman peaks at 957 and 987 cm^{-1} and in the thermal stabilisation of the PVDF-HFP component of the blend with added molybdenum trioxide, which increased the complex elastic modulus E^* over the entire temperature range.

A consistent and statistically significant antimicrobial activity of the polymer blend was observed only for the Gram-positive bacterium *L. monocytogenes*, but the polymer also reduced *S. aureus* for 0.5 log after 6 h of incubation. This is consistent with a report that the polymers are generally more active against Gram-positive bacteria due to the difference in cell membrane structure.[47] The PVDF-HFP/PVP/molybdenum trioxide nanocomposite proved to have good bactericidal activity, as it inactivated both Gram-positive and Gram-negative bacteria after 6 h of incubation. However, species-specific differences were observed in fungi, as the nanocomposite was fungicidal against yeast *P. anomala* and mould *P. verrucosum* but only reduced the number of yeast *C. albicans* and mould *A. flavus*. This can be explained by the optimal growth rate of *A. flavus* in the pH range of 3.5–6.0,[48] while *C. albicans* has the ability to adapt to changes in extracellular pH and colonise tissues with diverse pH in vivo.[49]

5. Conclusion

A novel nanostructured polymer composite was designed from inert biocompatible PVDF-HFP and water-soluble PVP polymers with incorporated molybdenum trioxide NWs. The nanofiller reduces the surface roughness, increases the wetting angle, changes the zeta potential from negative to positive, increases the thermal stability of the blend and preserves the polar β-phase in PVDF-HFP caused by the interaction between the two polymers. The high specific surface area of molybdenum trioxide NWs allows a fast dissolution and a consequent reduction in the pH value. The acidic environment enables hydrolysis of the PVP polymer, which could contribute to the antimicrobial function by forming carboxyl acid and ammonium salt. The synergy in the dissolving processes for PVP and molybdenum trioxide leads to sufficiently low pH values, although a relatively small amount of molybdenum trioxide (0.09 mg/ml in 1.5 h) is released from the nanocomposite. These characteristics indicate that the PVDF-HFP/PVP/molybdenum trioxide nanocomposite is a stable nanostructured coating that has a good antimicrobial potential and is unfavourable for colonisation by microorganisms. The advantage of the reported PVDF-HFP/PVP/molybdenum trioxide nanocomposite is the activation of its antimicrobial effect by water. Instead of using different disinfectants with different degrees of toxicity, which require frequent applications, the PVDF-HFP/PVP/molybdenum trioxide nanocomposite dissolves in water during the cleaning process or in water brought along by adhering microbes or condensed from the air humidity. The potential of its long-term antimicrobial and virucidal activity needs further investigation.

Acknowledgements

This work was financially supported by the Slovenian Research Agency through contracts P0-5544, P1-0099 and P4-0116. The authors thank Dr A. Abram for help with measurements of surface zeta potentials and static CAs and Dr L. Pirker for help in the synthesis of the molybdenum trioxide NWs. The authors thank in particular J. Žigon and Professor Dr M. Petrič for help with measurements of dynamic CAs.

REFERENCES

1. Satpathy S, Sen SK, Pattanaik S and Raut S (2016) Review on bacterial biofilm: an universal cause of contamination. *Biocatalysis and Agricultural Biotechnology* **7**: 56–66.
2. Palza H (2015) Antimicrobial polymers with metal nanoparticles. *International Journal of Molecular Sciences* **16**: 2099–2116.
3. Glinel K, Thebault P, Humblot V, Pradier CM and Jouenne T (2012) Antibacterial surfaces developed from bio-inspired approaches. *Acta Biomaterialia* **8**: 1670–1684.
4. Vasilev K, Cook J and Griesser HJ (2009) Antibacterial surfaces for biomedical devices. *Expert Review of Medical Devices* **6(5)**: 553–567.
5. Thome J, Holländer A, Jaeger W, Trick I and Oehr C (2003) Ultrathin antibacterial polyammonium coatings on polymer surfaces. *Surface and Coatings Technology* **174–175**: 584–587.
6. Greenhalgh R, Dempsey-Hibbert NC and Whitehead KA (2019) Antimicrobial strategies to reduce polymer biomaterial infections and their economic implications and considerations. *International Biodeterioration & Biodegradation* **136**: 1–14.

7. Ogunsona EO, Muthuraj R, Ojogbo E, Valerio O and Mekonnen TH (2020) Engineered nanomaterials for antimicrobial applications: a review. *Applied Materials Today* **18**: article 100473.
8. Guo L, Yuan W, Lu Z and Li CM (2013) Polymer/nanosilver composite coatings for antibacterial applications. *Colloids and Surfaces A: Physicochemical and Engineering Aspects* **439**: 69–83.
9. Schwartz VB, Thétiot F, Ritz S *et al.* (2012) Antibacterial surface coatings from zinc oxide nanoparticles embedded in poly(*N*-isopropylacrylamide) hydrogel surface layers. *Advanced Functional Materials* **22(11)**: 2376–2386.
10. Charpentier PA, Burgess K, Wang L *et al.* (2012) Nano-TiO_2/polyurethane composites for antibacterial and self-cleaning coatings. *Nanotechnology* **23**: article 425606.
11. Bondarenko O, Juganson K, Ivask A *et al.* (2013) Toxicity of Ag, CuO and ZnO nanoparticles to selected environmentally relevant test organisms and mammalian cells in vitro: a critical review. *Archives of Toxicology* **87(7)**: 1181–1200.
12. Shafaei S, Lackner M, Meier M *et al.* (2013) Polymorphs of molybdenum trioxide as innovative antimicrobial materials. *Surface Innovations* **1(4)**: 202–208, https://doi.org/10.1680/si.13.00021.
13. Zollfrank C, Gutbrod K, Wechsler P and Guggenbichler JP (2012) Antimicrobial activity of transition metal acid MoO_3 prevents microbial growth on material surfaces. *Materials Science and Engineering: C* **32**: 47–54.
14. Krishnamoorthy K, Veerapandian M, Yun K and Kim SJ (2013) New function of molybdenum trioxide nanoplates: toxicity towards pathogenic bacteria through membrane stress. *Colloids and Surfaces B: Biointerfaces* **112**: 521–524.
15. Kumar A and Pandey G (2017) Synthesis, characterization, effect of temperature on band gap energy of molybdenum oxide nano rods and their antibacterial activity. *American Journal of Applied and Industrial Chemistry* **3(3)**: 38–42.
16. Desai N, Mali S, Kondalkar V, Mane R and Hong C (2015) Chemically grown MoO_3 nanorods for antibacterial activity study. *Journal of Nanomedicine & Nanotechnology* **6**: 338–344.
17. Chaves-Lopez C, Nguyen HN, Oliveira RC *et al.* (2018) A morphological, enzymatic and metabolic approach to elucidate apoptotic-like cell death in fungi exposed to h- and α-molybdenum trioxide nanoparticles. *Nanoscale* **10(44)**: 20702–20716.
18. Laxmayyaguddi Y, Mydur N, Shankar Pawar A *et al.* (2018) Modified thermal, dielectric, and electrical conductivity of PVDF-HFP/$LiClO_4$ polymer electrolyte films by 8 MeV electron beam irradiation. *ACS Omega* **3**: 14188–14200.
19. Sundaram NTK and Subramania A (2007) Microstructure of PVdF-*co*-HFP based electrolyte prepared by preferential polymer dissolution process. *Journal of Membrane Science* **289(1–2)**: 1–6.
20. Malmonge LF, Malmonge JA and Sakamoto WK (2003) Study of pyroelectric activity of PZT/PVDF-HFP composite. *Materials Research* **6(4)**: 469–473.
21. Cao JH, Zhu BK and Xu YY (2006) Structure and ionic conductivity of porous polymer electrolytes based on PVDF-HFP copolymer membranes. *Journal of Membrane Science* **281**: 446–453.
22. Shawky AI, Noor MJMM, Nasef MM *et al.* (2016) Enhancing antimicrobial properties of poly(vinylidene fluoride)/hexafluoropropylene copolymer membrane by electron beam induced grafting of *N*-vinyl-2-pyrrolidone and iodine immobilization. *RSC Advances* **6**: 42461–42473.
23. Guo Z, Xu X, Xiang Y, Lu SA and Jiang SP (2015) New anhydrous proton exchange membranes for high-temperature fuel cells based on PVDF–PVP blended polymers. *Journal of Materials Chemistry A* **3(1)**: 148–155.
24. Wang M, Fang D, Wang N *et al.* (2014) Preparation of PVDF/PVP core–shell nanofibers mats via homogeneous electrospinning. *Polymer* **55**: 2188–2196.
25. Yao C, Li X, Neoh KG, Shi Z and Kang ET (2009) Antibacterial activities of surface modified electrospun poly(vinylidene fluoride-*co*-hexafluoropropylene) (PVDF-HFP) fibrous membranes. *Applied Surface Science* **255(6)**: 3854–3858.
26. Varlec A, Arčon D, Škapin SD and Remškar M (2016) Oxygen deficiency in MoO_3 polycrystalline nanowires and nanotubes. *Materials Chemistry and Physics* **170**: 154–161.
27. Božinović K, Nestić D, Gradišar Centa U *et al.* (2020) In-vitro toxicity of molybdenum trioxide nanoparticles on human keratinocytes. *Toxicology* **444**: article 152564.
28. Zhang Y, Yang M, Portney NG *et al.* (2008) Zeta potential: a surface electrical characteristic to probe the interaction of nanoparticles with normal and cancer human breast epithelial cells. *Biomedical Microdevices* **10**: 321–328.
29. Wilhelmy J (1863) Über die Abhängigkeit der Kapillaritäts-Konstanten des Alkohols von Substanz und Gestalt des Benetzten Festen Körpers. *Annalen der Physik* **119**: 177–217 (in German).
30. Ström G, Fredriksson M and Stenius P (1987) Contact angles, work of adhesion, and interfacial tensions at a dissolving Hydrocarbon surface. *Journal of Colloid and Interface Science* **119(2)**: 352–361.
31. ISO (International Organization for Standardization) (2007) ISO 22196:2007: Plastics – measurement of antibacterial activity on plastics surfaces. ISO, Geneva, Switzerland.
32. Kalampounias AG, Tsilomelekis G, Berg RW and Boghosian S (2012) Molybdenum(VI) oxosulfato complexes in MoO_3–$K_2S_2O_7$–K_2SO_4 molten mixtures: stoichiometry, vibrational properties, and molecular structures. *Journal of Physical Chemistry A* **116(35)**: 8861–8872.
33. Sharma RK and Reddy GB (2014) Synthesis and characterization of α-MoO_3 microspheres packed with nanoflakes. *Journal of Physics D: Applied Physics* **47(6)**: article 065305.
34. Singh P, Borkar H, Singh BP, Singh VN and Kumar A (2014) Ferroelectric polymer–ceramic composite thick films for energy storage application. *AIP Advances* **4**: article 087117.
35. Beattie IR and Gilson TR (1969) Oxide phonon spectra. *Journal of the Chemical Society A: Inorganic, Physical, Theoretical* **969**: 2322–2327.
36. Dieterle M and Mestl G (2002) Raman spectroscopy of molybdenum oxides. *Physical Chemistry Chemical Physics* **4**: 822–826.
37. Turner DT and Schwartz A (1985) The glass transition temperature of poly(*N*-vinyl pyrrolidone) by differential scanning calorimetry. *Polymer* **26**: 757–762.
38. Remškar M, Iskra I, Jelenc J *et al.* (2013) A novel structure of polyvinylidene fluoride (PVDF) stabilized by MoS_2 nanotubes. *Soft Matter* **9**: 8647–8653.
39. Strobel M and Lyons CS (2011) An essay on contact angle measurements. *Plasma Processes and Polymers* **8(1)**: 8–13.
40. Manoudis PN and Karapanagiots I (2013) Modification of the wettability of polymer surfaces using nanoparticles. *Progress in Organic Coatings* **77**: 331–338.
41. Juárez-Moreno JA, Ávila-Ortega A, Oliva AI and Cauich-Rodríguez JV (2015) Effect of wettability and surface roughness on the adhesion properties of collagen on PDMS films treated by capacitively coupled oxygen plasma. *Applied Surface Science* **349**: 763–773.
42. Cai K, Bossert J and Jandt KD (2006) Does the nanometre scale topography of titanium influence protein adsorption and cell proliferation? *Colloids and Surfaces B: Biointerfaces* **49(2)**: 136–144.
43. Taylor RL, Verran J, Lees GC and Ward AJP (1998) The influence of substratum topography on bacterial adhesion to polymethyl methacrylate. *Journal of Materials Science: Materials in Medicine* **9**: 17–22.
44. Oliveira R, Azeredo J, Teixeira P and Fonseca AP (2001) The role of hydrophobicity in bacterial adhesion. In *Biofilm Community Interactions: Chance or Necessity?* (Gilbert P, Allison D, Brading M, Verran J and Walker J (eds)). BioLine, Cardiff, UK, pp. 11–22. See http://citeseerx.ist.psu.edu/viewdoc/download?doi=10.1.1.625.340&rep=rep1&type=pdf (accessed 11/12/2020).

45. Manna S and Nandi AK (2007) Piezoelectric β polymorph in poly (vinylidene fluoride)-functionalized multiwalled carbon nanotube nanocomposite films. *Journal of Physical Chemistry C* **111**: 14670–14680.
46. Frank HP (1954) The lactam-amino acid equilibria for ethylpyrrolidone and polyvinylpyrrolidone. *Journal of Polymer Science* **12**: 565–576.
47. Tashiro T (2001) Antibacterial and bacterium adsorbing macromolecules. *Macromolecular Materials and Engineering* **286**: 63–87.
48. Kosegarten CE, Ramírez-Corona N, Mani-López E, Palou E and López-Malo A (2017) Description of *Aspergillus flavus* growth under the influence of different factors (water activity, incubation temperature, protein and fat concentration, pH, and cinnamon essential oil concentration) by kinetic, probability of growth, and time-to-detection models. *International Journal of Food Microbiology* **240**: 115–123.
49. Davis D (2003) Adaptation to environmental pH in *Candida albicans* and its relation to pathogenesis. *Current Genetics* **44**: 1–7.